

Desert dust aerosol age characterized by mass-age tracking of tracers

Qin Han¹ and Charles S. Zender¹

Received 6 March 2010; revised 1 August 2010; accepted 10 August 2010; published 16 November 2010.

[1] We introduce and apply to dust aerosols an efficient method to track tracer age (time since emission) as a function of space and time in large-scale geophysical models. Our mass-age tracking (MAT) method follows the full tracer lifecycles directly and does not depend on proxy, ensemble, or Green's function techniques. MAT sends a mass-age tracer through the same algorithms that the host models use to predict tracer mass processes and then estimates age as the ratio of mass-age to mass. We apply MAT to size-resolved dust aerosol tracers to study the age of dust that remains in the atmosphere and the age of dust at deposition. The results include the first global distribution maps of aerosol age. Dust age varies with location, time, and particle size and is strongly sensitive to climate, wind and precipitation in particular. The global average age of dust at deposition agrees with residence time at ~ 2.7 days, while dust in the atmosphere is, on average, twice as old. As expected, older dust prevails far from sources, at higher altitudes and in smaller sizes. Dust age exhibits a seasonal cycle, stronger for larger dust particles, that peaks in April–June, the period of maximum Asian and North African emissions. The oldest dust at deposition falls in the Antarctic and South Pacific Convergence Zone about 1 month after emission. The mass-weighted ages provided by MAT are useful for investigating and parameterizing the evolution of aerosol physical and chemical properties.

Citation: Han, Q., and C. S. Zender (2010), Desert dust aerosol age characterized by mass-age tracking of tracers, *J. Geophys. Res.*, 115, D22201, doi:10.1029/2010JD014155.

1. Introduction

[2] Atmospheric aerosols have large impacts on climate, biogeochemistry and human health and these impacts often depend on the aerosol age, i.e., time since emission/formation. From the moment an aerosol forms or is emitted until its deposition, its composition, phase, and even shape may change to maintain thermodynamic and chemical equilibrium with the environment. This “aging” can modify the aerosol scattering and absorption properties which determine its direct radiative effects, i.e., perturbations of the solar and terrestrial radiation fields, as well as its indirect radiative effects through influencing cloud properties. Aerosol solubility is a crucial factor in atmospheric delivery of bioavailable ocean nutrients and micronutrients (e.g., Fe) to which ocean biogeochemistry is sensitive [Krishnamurthy *et al.*, 2009]. Solubility depends on atmospheric processes (trace gas exposure, heterogeneous and photochemistry, cloud processing) during transport [Spokes and Jickells, 1996; Hand *et al.*, 2004; Luo *et al.*, 2005]. Age-based parameterization of solubility can be estimated from field measurements with the aid of back trajectory models

[Hand *et al.*, 2004; Buck *et al.*, 2008], and from models that represent solubility as a diffusive or surface-area-controlled process with known time constants (Han *et al.*, manuscript in preparation). Knowing the duration of aerosol transport, i.e., the aerosol age, can help us understand and thereby better predict or parameterize the age-related change in aerosol physical and chemical properties [e.g., Hand *et al.*, 2004; Luo *et al.*, 2008]. Here we introduce and apply to dust aerosols an efficient method to track tracer age in large-scale geophysical models.

[3] Aerosol age differs from aerosol lifetime (residence time). The former is the time since emission/formation, while the latter is the average time that aerosols remain in the atmosphere and is defined as the mean atmospheric burden divided by the total mean source or sink [Prather, 2007]. Age and residence time are closely related in that the global mean mass-weighted aerosol age at deposition asymptotes to the residence time as aerosol sources and sinks approach equilibrium. Many studies have estimated the residence times of various aerosols using this definition. Global mean aerosol residence times vary from just a few hours for large ($>5 \mu\text{m}$ diameter) aerosols such as mineral dust, to more than 2 weeks for submicron fine aerosols [e.g., Zender *et al.*, 2003; Mahowald *et al.*, 2006]. Aerosol residence time can also be estimated from the decay of radioactive tracers both measured [Kuroda *et al.*, 1962; Poet *et al.*, 1972] and in models [Seinfeld and Pandis, 2006]. However,

¹Department of Earth System Science, University of California, Irvine, California, USA.

global mean residence times conceal the great spatiotemporal variations of atmospheric lifetime that arise from local variations in meteorology and deposition processes (gravitational, turbulent, and wet deposition, i.e., washout). The time since emission of aerosols in a given air parcel is more relevant to their instantaneous radiative and chemical influence than is their expected residence time.

[4] The age of nonradioactive tracers is difficult to measure and to calculate because it depends on the history of an air parcel (or mixture of air parcels) rather than on a global mean budget. Unlike gaseous tracers (e.g., ozone, CO), aerosols experience net motion (e.g., gravitational settling) relative to their air parcel of origin and this complicates their age determination.

[5] Previous studies have estimated tracer age in different ways including the use of age proxies. One early approach estimated the “photochemical age” of an air mass from the ratio of hydrocarbons [Roberts *et al.*, 1984]. This approach neglects reactions with oxidants other than OH so that the “photochemical age” relies on the OH concentrations and does not change when the OH concentrations are low. Other assumptions, including that the hydrocarbons used have the same sources, that the sources have a constant compound composition and that the background concentrations are negligible, also make this method inaccurate [Roberts *et al.*, 1984; Parrish *et al.*, 1993; McKeen and Liu, 1993]. A newer proxy-based approach relies on the differing reaction rates of various stable isotopic counterparts of the same hydrocarbon, rather than the reaction rates from two hydrocarbons and OH [Rudolph and Czuba, 2000]. This method makes fewer assumptions and can estimate the average age of each hydrocarbon. However, both of these proxy-based approaches rely on hydrocarbon reaction rates and neither of them applies well to other aerosol species.

[6] Previous models have implemented “Age tracer” to track the time since a given seawater parcel was last exposed to the atmosphere, aka the ventilation age [e.g., Thiele and Sarmiento, 1990; England, 1995]. This method constructed the continuity equations for age tracers and the age is incremented by one time step during each time step. Similar method has been used to track the age of air [e.g., Neu and Plumb, 1999]. It is possible to apply this method to tracers. However, each tracer requires its own continuity equation, so this method is not readily generalizable.

[7] More recent research uses additional tracers in trajectory models to track aerosol age distributions [e.g., Kleinman *et al.*, 2003; Stohl *et al.*, 2003]. Tracers are tagged to track the emission time and have the same chemical reaction rates as the aerosols that they track [Kleinman *et al.*, 2003]. This approach neglects the mixing of air masses with different ages and looks at only the age of aerosols emitted into the air parcel during the modeled period. Another approach with a Lagrangian trajectory model estimates CO age distribution by tracking the transport time and the contribution from source grids. Though backward simulations yield a higher space and time resolution than the corresponding forward simulations, the age distributions calculated by parcel trajectory methods are typically limited by (1) simplified chemistry, (2) simulation of one pathway per parcel (which can be ameliorated by ensemble techniques as discussed below).

[8] The preceding age-tracking methods have drawbacks in that they (1) rely on particular emission compositions, (2)

are not easily extensible to other aerosol species, and (3) do not account for the mixing of air masses with different ages. General Circulation Models (GCMs) and/or Chemical Transport Models (CTMs) with more complete aerosol schemes can solve most of these problems by utilizing the details of transport and deposition processes. Krinner and Genthon [2003] used idealized radioactive tracers to analyze tracer age at any given place in an atmospheric GCM. Radioactive decay was used as the only sink, and was intended to implicitly approximate the net removal time scale by all processes. However, the aerosol ages obtained depend on the lifetime assumed for the radioactive tracer whereas the aerosol ages should be independent of the radioactive tracer used.

[9] The age distribution of an aerosol population is best described by a Probability Density Function (PDF). Ensemble and Green’s Function methods can be used separately and together to determine the PDF of aerosol ages (and trajectories). Waugh *et al.* [2003] used the Transit-time PDF (TTPDF) method [Hall and Plumb, 1994; Holzer and Hall, 2000] to examine the ages of different tracers as well as the temporal variations in tracer ages. Holzer *et al.* [2003] applied the same method to a CTM to analyze springtime trans-Pacific atmospheric transport from east Asia. Primeau and Holzer [2006] used a similar technique to track the tracer-independent ventilation rates and the global ocean age inventory. The TTPDF method yields the transit time distributions within a grid box and thus calculates mean tracer ages accurately. However, this method requires a large ensemble of simulations when tracking age in time-varying flow fields.

[10] Wagstrom and Pandis [2009] used the Particulate Matter Source Apportionment Technology (PSAT) to track the aerosol age in a CTM. The emissions were grouped into bins based on the time of emission. Each of these emission time periods (ETPs) was treated as a source category by PSAT. Then the average age of any aerosol species at a particular location and time was estimated using the mass contributions from each bin and the average age of each bin. This method is good for estimating average age of aerosols in a short time period. Though the ETP has only a mild impact on the age estimation, the number of the ETPs could be very large for long-term runs so that the computational time increases unreasonably.

[11] Our motivation for developing MAT stems from our efforts to model the effects of atmospheric aerosols on ocean biogeochemistry [Han *et al.*, 2008; Krishnamurthy *et al.*, 2009]. For this purpose, we needed an age-tracking method to satisfy the following requirements that, collectively, are not met by any of the previous methods: firstly, it runs online in GCMs/CTMs so that instantaneous (rather than climatological) tracer age is always known and can be coupled between atmosphere and ocean; secondly, it is computationally inexpensive; thirdly, it is generic and applies to any tracer simulated; fourthly, it gives mean mass-weighted ages (which may be empirically related to aerosol solubility); lastly, it is deterministic and reproduces the same ages for any given meteorology and tracer physics.

[12] Our mass-age tracking (MAT) method satisfies these requirements. It requires one additional tracer, for mass-age, per tracer species, and yields results online, during a single simulation rather than requiring postprocessing of an

Table 1. Dust Ages and Residence Times (in Days) in Equilibrium Present-Day Climate^a

Size Bin	Dust Diameter (μm)	MATCH ^b Global Mean τ	CAM Global			CAM Northern Hemisphere			CAM Southern Hemisphere		
			τ	α_{dps}	α_{wet}	α_{dry}	α_{air}	α_{dps}	α_{air}	α_{dps}	α_{air}
Bin1	0.1–1.0	16.9	7.8 ± 0.2	7.8 ± 0.2	7.9 ± 0.2	3.9 ± 0.1	8.4 ± 0.1	7.6 ± 0.2	7.9 ± 0.1	9.2 ± 0.4	12.3 ± 0.3
Bin2	1.0–2.5	10.9	7.3 ± 0.2	7.2 ± 0.2	7.6 ± 0.2	3.9 ± 0.2	7.1 ± 0.1	7.0 ± 0.2	6.86 ± 0.09	8.4 ± 0.4	9.0 ± 0.3
Bin3	2.5–5.0	3.5	3.8 ± 0.1	3.7 ± 0.1	6.1 ± 0.1	1.82 ± 0.08	5.40 ± 0.06	3.6 ± 0.1	5.30 ± 0.06	4.5 ± 0.1	6.2 ± 0.1
Bin4	5.0–10.0	1.1	1.37 ± 0.04	1.37 ± 0.04	3.7 ± 0.1	0.92 ± 0.03	3.15 ± 0.05	1.34 ± 0.04	3.11 ± 0.06	1.67 ± 0.03	3.44 ± 0.05
All sizes	0.1–10.0	4.3	2.69 ± 0.06	2.67 ± 0.07	5.9 ± 0.2	1.10 ± 0.04	5.47 ± 0.08	2.56 ± 0.07	5.30 ± 0.07	3.7 ± 0.2	6.9 ± 0.2

^aAbbreviations: τ is residence time, α_{dps} is age at deposition, α_{wet} is age at wet deposition, α_{dry} is age at dry deposition, and α_{air} is age of dust aloft.

^bGlobal mean residence time (in days) from Zender *et al.* [2003].

ensemble of simulations. Though the MAT method cannot compute the age PDFs for each grid cell, it estimates the mass-weighted mean aerosol ages accurately and is computationally efficient. In this work, we apply MAT to investigate the age distributions in the atmosphere and at deposition of four sizes of dust aerosol.

2. Method

[13] The MAT method is generic and may be implemented in any geophysical model with grid-based (Eulerian) representation of mass-conserving tracer physics and dynamics. In this work we apply MAT to wind generated desert dust, motivated by questions of atmospheric nutrient deposition to understand the age and solubility of aerosol at deposition [Spokes and Jickells, 1996; Hand *et al.*, 2004]. The host GCM is the National Center for Atmospheric Research (NCAR) Community Atmosphere Model, version 3 (CAM3) [Collins *et al.*, 2004], configured as in Flanner *et al.* [2007].

[14] The dust source, transport and deposition mechanisms follow the Dust Entrainment and Deposition Module (DEAD) [Zender *et al.*, 2003]. Dust is entrained into the atmosphere through wind mobilization and removed by dry gravitational settling, turbulent dry deposition and wet deposition during precipitation events. Between the sources and sinks, dust is advected and diffused as a passive tracer by the transport processes used in CAM3, including vertical diffusion, shallow convection, deep convection and semi-Lagrangian tracer transport. Dust is divided into four size bins based on the diameters of the particles (Table 1) and particle size distributions are assumed to be time-invariant within each bin. A dust particle does not change its effective size or mass through its lifecycle and there is no exchange between bins.

[15] The implementation of the MAT method is straightforward. For each tracer species in the host model (e.g., GCM or CTM), MAT prognoses one additional tracer: the mass-age (the product of aerosol mass and age, in units of [kg s]) of the tracer. In this case, the mass-age of each dust aerosol size class is carried through each lifecycle process mentioned above at all model grid points and the mass-weighted age (A) of dust aerosols is then derived by dividing mass-age (mA) by mass (m). If we describe the change of dust dry mass in the model as

$$\frac{dm}{dt} = \mathcal{L}(m) + S, \quad (1)$$

then the change of dust mass-age can be described as

$$\frac{dmA}{dt} = \mathcal{L}(mA) + m \times T, \quad (2)$$

where S is the dust source from wind mobilization, T is the length of time for one model time step (20 minutes in our case), and the operator \mathcal{L} denotes all other dust lifecycle processes including vertical diffusion, shallow convection, deep convection, semi-Lagrangian tracer transport, and dry and wet deposition. Previous age tracer methods [Thiele and Sarmiento, 1990; England, 1995; Neu and Plumb, 1999]

track tracer age by solving a separate prognostic equation for A (not mA as in equation (2)) for each tracer. The elegance of MAT is that the lifecycle operator \mathcal{L} is the same for mass and mass-age, so that the same algorithms and codes used on tracer mass can be reused on mass-age. There are exceptions, discussed below, for algorithms that contain mass-specific switches. Both dust mass (m) and mass-age (mA) are zero initially and they also have the same sinks (wet and dry deposition). The only difference is that the source of dust mass is emission, while the source of mass-age is the internal increment of one time step per unit mass during each time step. Note that we use dust to demonstrate the use of MAT for an inert tracer. MAT applies to other tracers, even to chemically and thermodynamically active species, as long as all the processes are included in the operator \mathcal{L} .

[16] If the host model conserves tracer mass then it will conserve tracer mass-age too, either automatically, or after some coaxing described below. In equilibrium, the global total mass-age deposited in a period equals the total mass-age added in the same period. The former is the product of global mean mass-weighted age of dust at deposition and the mass of dust deposited in this period. The latter is the product of the mass of dust that remains in the atmosphere and the length of this period. Thus, by definition, the global average mass-weighted age of deposited dust equals the global dust residence time at equilibrium.

[17] We uncovered one obstacle to accurate implementation of MAT by verifying the conservation of the mass-age tracer. To wit, dynamic and physical process algorithms (e.g., advection, wet deposition) often contain nonlinear switches or conditions (if-then statements) that depend on the tracer value being in the expected range. Such conditions might be that tracer mixing ratio and mass should not be negative, or that tracer mixing ratio should exceed some small value (ϵ ($\epsilon \sim 10^{-30}$)) so that floating point arithmetic will not underflow in single precision. Small differences arise when these algorithms encounter the mass-age tracer since the same numerical limit has different effects on mass than on mass-age by the factor A (i.e., $A \sim 3 \times 10^7$ seconds or $A \sim 26280$ time steps for an 1 year old tracer). Fortunately these problems usually occur only in “corner cases” such as extremely low mass concentrations where the simple mass approximations are acceptable because they affect negligible mass and mass-age. Ensuring the consistent ordering of time-split processes for both mass and mass-age is also important. We solve this problem by making consistent approximations to the mass-age tracer as to mass. For example, we had to change the CAM convection physics algorithm from “if mass is negative, replace it with the (positive-definite) values from the preceding time-split process (PV)” to “if mass or mass-age is negative, replace it with PV” for the mass-age tracer, so that both mass and mass-age follow the same code path. Hence in our implementation of MAT, the mass-age tracers are conserved to the same precision as the mass tracers.

[18] Here we use MAT to track the mass-weighted age of dust that remains in the atmosphere (for conciseness, referred to hereafter as dust aloft), and of dust deposited to the surface as functions of space, time, and dust size. The results shown below are averages and time series from the

last 10 years of 20 year equilibrium present-day climate simulations.

3. Results: Dust Age in Present-Day Climate

3.1. Temporal Evolution of Dust Age and Residence Time

[19] Dust lifetime, which as mentioned above, is also known as its residence time, is the average time that dust particles are expected to stay in the atmosphere and is defined as the total global dust burden in the atmosphere divided by the dust deposition (or mobilization) rate. Dust age is defined as the time elapsed since a dust particle entered the atmosphere and is computed by MAT. Average dust residence times range from 1.5 to 8.2 days from the largest dust sizes modeled (5–10 μm diameter) to the smallest submicron dust sizes (Table 1). The residence times compare well with Mahowald *et al.* [2006] who also used the CAM GCM. Residence times computed from the dust field simulated by the MATCH CTM and driven by National Center for Environment Prediction (NCEP) analyzed meteorology for the period 1990–1999 [Zender *et al.*, 2003] differ from the residence times calculated from CAM. The long-term average residence time in MATCH is more than twice the CAM residence time for bin 1 and is ~ 3 days longer for bin 2. For bins 3 and 4, the MATCH residence times are slightly shorter than those from CAM. These differences arise because MATCH and CAM have slightly differing dust entrainment and deposition schemes, and strongly differing meteorologies, in particular wind and precipitation. The residence times for small dust particles are more sensitive to the meteorology than those for large dust particles, because smaller dust particles are more susceptible to long range transport and wet scavenging. MATCH and CAM utilize different horizontal resolutions which would also produce differing dust fields [Zender *et al.*, 2004].

[20] The ages of dust aloft and of dust at deposition both decrease as the particle size increases. The MAT-calculated global average ages of deposited dust and the traditional residence times are not identical but agree as well as expected (Table 1, Figure 1). The small differences between them reflect the ever changing atmospheric dust burden. Approximations made in CAM to conserve mass in a positive-definite manner [Collins *et al.*, 2004] and approximations we make to conserve mass-age could also contribute to these differences. Dust aloft is usually 1–2 days older than dust at deposition except for size bin 2 (1–2.5 μm diameter). As discussed below, this is due to size-dependent deposition processes and ages.

[21] The residence times and ages of dust at deposition have strong annual cycles with longer ages/residence times in Northern Hemisphere (NH) spring/summer (Figure 1). The seasonal cycles of residence times and ages at deposition of smaller dust have a sharp drop following the annual maximum. The residence times and ages at deposition of larger dust drop more slowly and the minima are seen in NH winter. The ages of all sizes of dust aloft have clear seasonal cycles except the age of submicron (size bin 1) dust aloft. The seasonal cycles of dust ages and residence times are probably caused by the seasonal changes of dust plume locations and of precipitation near the plumes. However, it

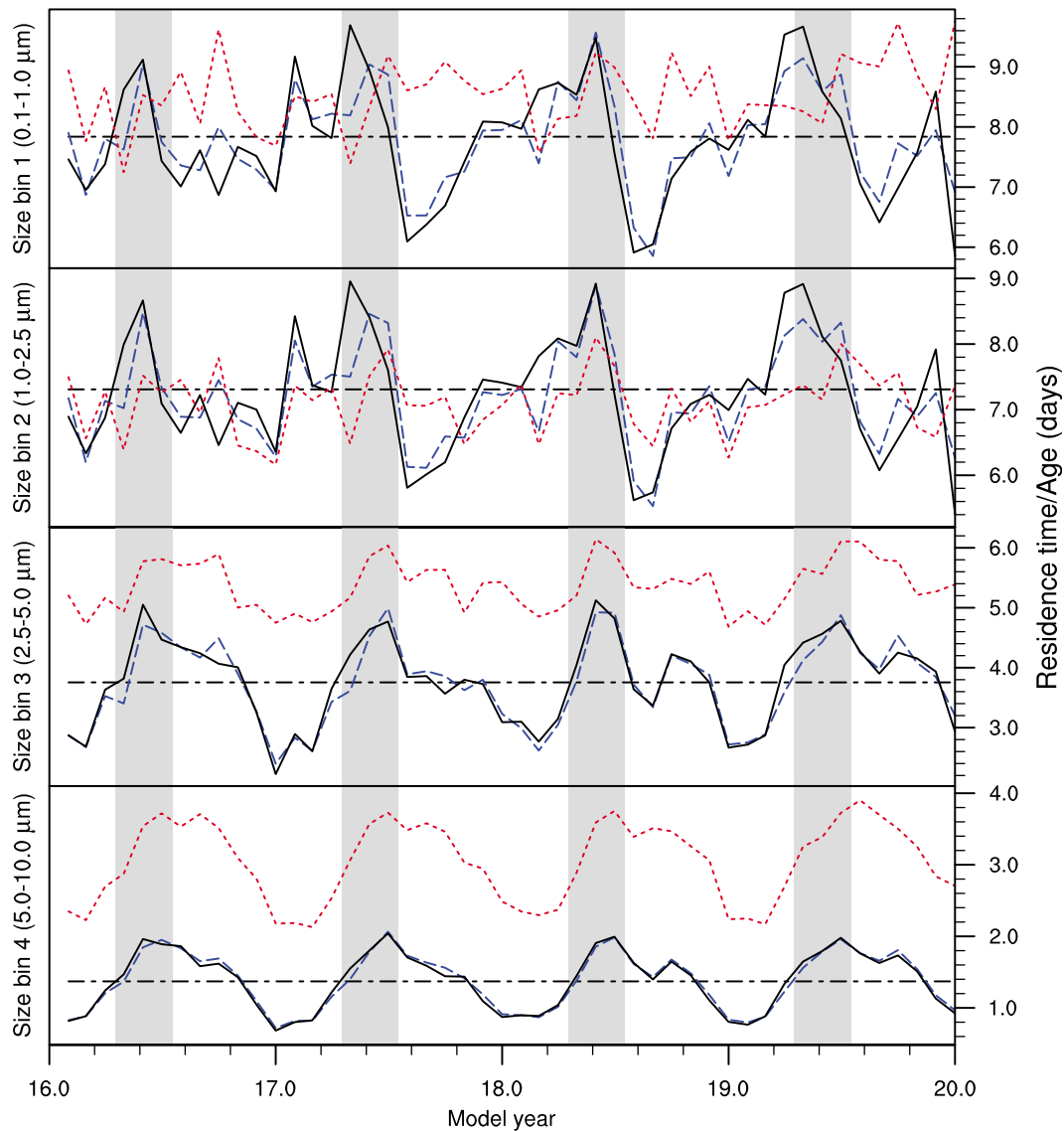


Figure 1. Global mass-weighted average ages of dust in the atmosphere (red dotted line), ages of dust at deposition (blue dashed line), and dust residence times (black solid line) as a function of time (model year 17–20) for four dust sizes. The black dash-dotted lines show the average residence times. Gray area denotes April, May, and June in each year.

is not clear why the seasonal patterns are different for different dust sizes.

3.2. Spatial Distribution of Dust Age

3.2.1. Age at Deposition and Aloft

[22] The MAT method reveals the mass-weighted ages of dust at deposition globally (Figures 2a and 2b). Dust is relatively young when deposited near source regions and is relatively old when deposited far from source regions. Dust deposited at inland deserts in low and middle latitudes ranges in age from 1 to 2 days old (submicron dust) to only a few hours (5–10 μm). Dust deposited to remote oceans and to polar regions is more than 2 weeks old (size bin 1) and more than 1 week old (size bin 4). Note that the largest dust settles relatively quickly ($\sim 300 \text{ m d}^{-1}$) so that mass fraction (and mass flux) of this dust that is older

than 1 week is extremely small. Oceans downwind of dust source regions, such as the equatorial Atlantic, receive intermediate-aged dust. The Southern Hemisphere (SH) receives older deposited dust than the NH since the SH is relatively farther from dust sources. The global average age of dust at deposition is much closer to the NH than the SH age since the NH deposition rate is 10 times more than the SH rate and we report the mass-weighted age. Of course in terms of chemical processing and effects on solubility it is the local not the global mass-weighted ages that matter.

[23] The age of dust aloft is also derived by using the mass-age tracers. The dust ages increase with height and, as expected, modeled dust in the stratosphere is much older than in the troposphere: more than 2 years for submicron dust and 2–3 months for 5–10 μm dust (Figure 3).

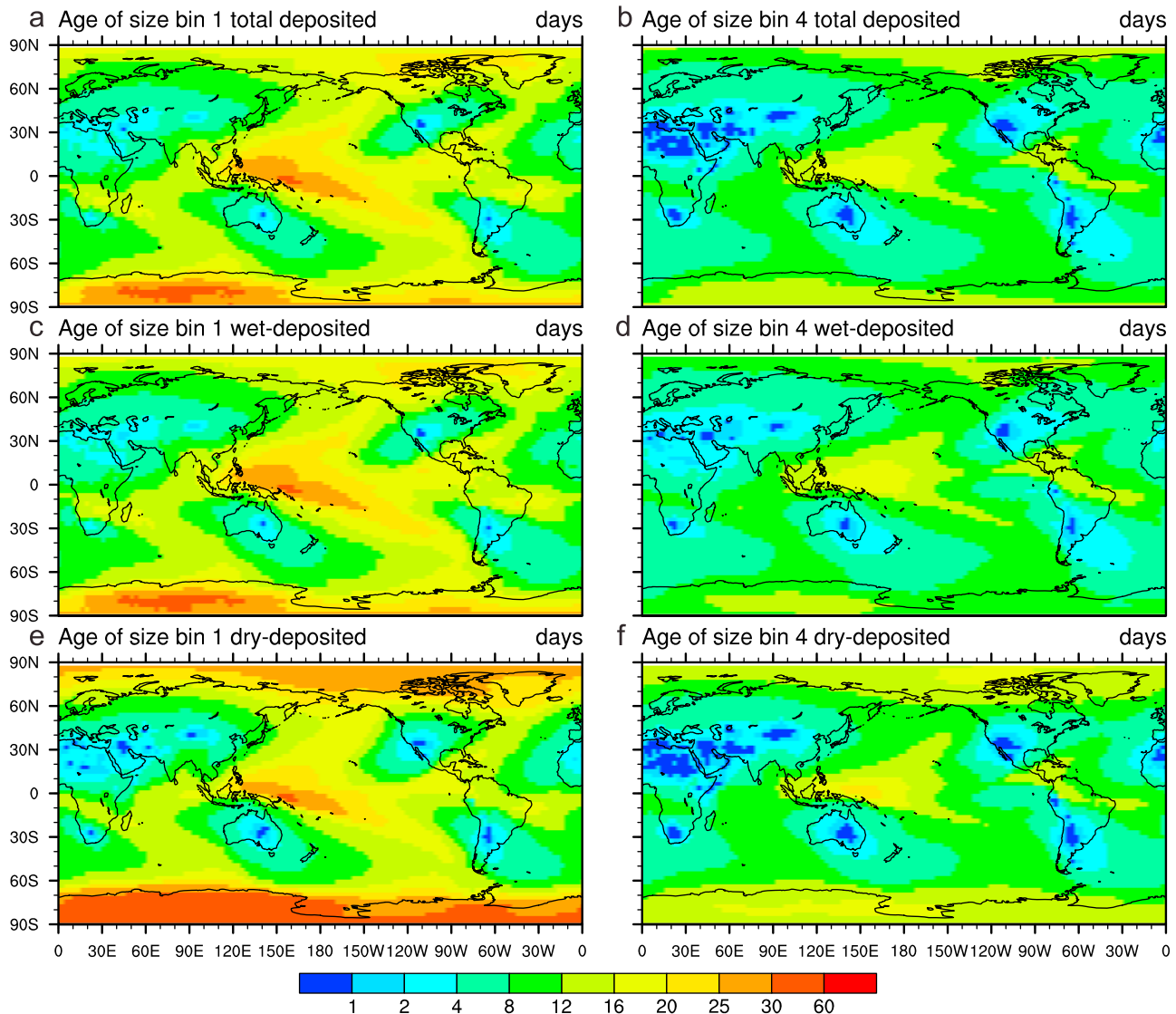


Figure 2. Spatial distributions of deposited dust ages (days) averaged through the last 10 model years: (a) ages of total (wet + dry) deposited submicron (size bin 1) dust, (b) ages of total deposited 5–10 μm (size bin 4) dust, (c) ages of wet-deposited size bin 1 dust, (d) ages of wet-deposited size bin 4 dust, (e) ages of dry-deposited size bin 1 dust, and (f) ages of dry-deposited size bin 4 dust.

Note that the CAM GCM employed is primarily a tropospheric GCM so distributions of tracers in the stratosphere should not be over-interpreted. The ages of dust near the surface are consistent with the ages of deposited dust. Dust deposited around 30°N ages since the dominant dust sources (subtropical deserts) are located there. Polar regions have old dust ages since they are very far from dust sources.

3.2.2. MAT Modified to Diagnose Spatial Trajectories

[24] The oldest dust deposited outside the Antarctic falls in the equatorial Pacific region (0–10°S) along the South Pacific Convergence Zone (SPCZ). Dust falling in this region northeast of Australia (Figure 2) can be more than one month old. The atmospheric dust aloft at 10°S is also ~5 days older than the surroundings (Figure 3). We examined the extent to which dust passing through the strato-

sphere contributes to the old age of the dust in this region. Before we get into this discussion, we caution that very little dust falls there. Thus the age of SPCZ dust is of interest for processes which strongly depend on the tail of the aerosol age distribution.

[25] At least two competing hypotheses could explain the great mass-weighted age of SPCZ dust. First, the age may be influenced by dust that entered the upper troposphere or lower stratosphere in deep convective events, and exited likewise or through settling. It could also be dust that was emitted from North America and Africa and transported by slow easterlies in the equatorial boundary layer. We are unaware of any measurement of dust aerosol ages in the SPCZ region.

[26] Estimating how much tracer traverses a given spatial region requires only a slight modification of the MAT

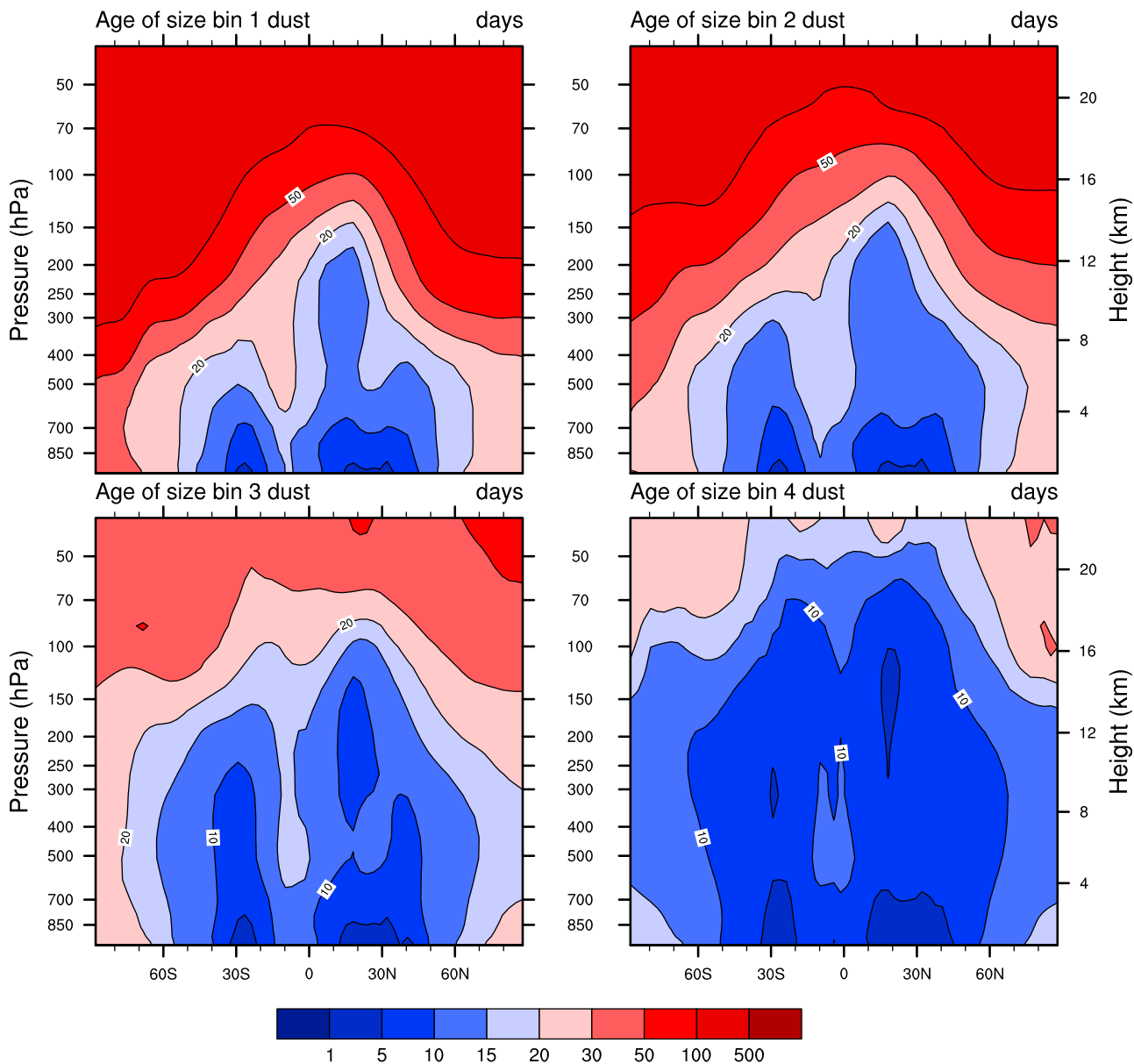


Figure 3. Vertical and meridional age distributions (days) for four sizes of dust in the atmosphere averaged through the last 10 model years.

method. We track the mass of dust that has been to the stratosphere (mf) by

$$\frac{dmf}{dt} = \mathcal{L}(mf), \quad (3)$$

where mf is initially zero everywhere and then equals the total dust mass (m) for any stratospheric region (defined to be above the model interface at 92 hPa since the tropical tropopause is normally below 100 hPa). Here mf is conserved once created by dust mass that enters the stratosphere by rising above the 92 hPa model level. The mean mass-weighted fraction of dust that has been to the stratosphere (f) thus equals the ratio of mf to m .

[27] Thus the modified MAT estimates the fraction of dust that has ascended, at least once, above 92 hPa. This is a

conservative estimate (lower bound) of the fraction of dust that has been in the stratosphere (Figures 4a and 4b) since the tropopause at higher latitudes is usually much lower than 92 hPa taken to demarcate the tropical tropopause. We caution that although the cross-tropopause transport (e.g., deep convection) in CAM has been evaluated [Rasch *et al.*, 2006; Williamson and Rasch, 1994], whether the fluxes of aerosols by this transport are correctly represented remains unclear. Less than 5% of the smallest dust particles and less than 0.5% of the largest dust particles deposited in the SPCZ traversed the stratosphere. We also traced dust that rose above 208 hPa and found that more than 40% of submicron dust and more than 50% of 5–10 micron dust deposited in the SPCZ traversed the upper troposphere lower stratosphere (UTLS) region between 92 hPa and 208 hPa (Figures 4c and

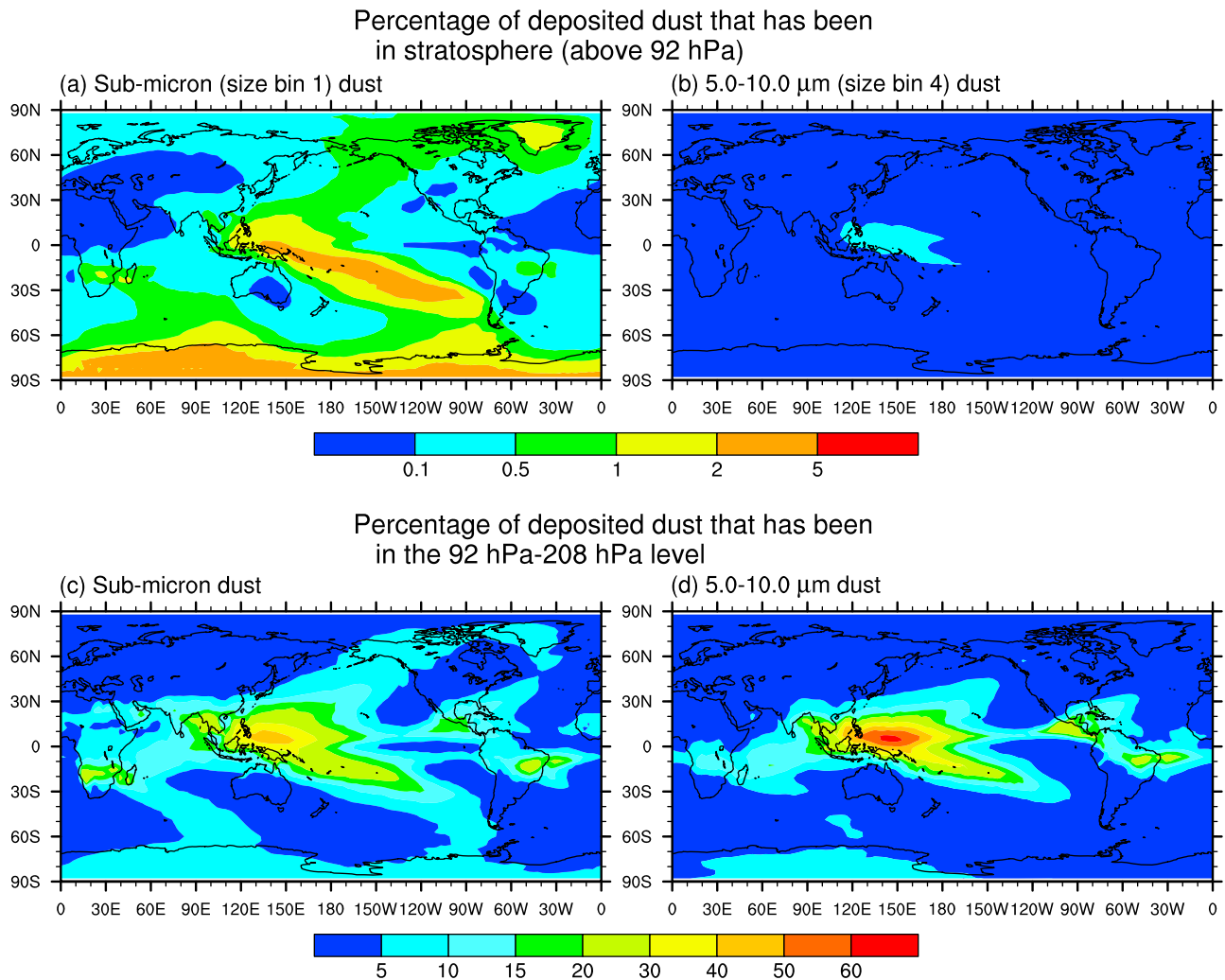


Figure 4. The percentage of deposited dust that has been (a) above 92 hPa for submicron (size bin 1) dust, (b) above 92 hPa for 5–10 μm (size bin 4) dust, (c) between 92 and 208 hPa for submicron dust, and (d) between 92 and 208 hPa for 5–10 μm dust.

4d). The large fraction of UTLS dust explains well the old mass-weighted ages of the deposited dust in the SPCZ. Strong and deep convective events can explain why the SPCZ has the largest fraction of stratosphere-influenced dust. It is unclear why the intertropical convergence zone (ITCZ) to the north does not follow the same pattern.

3.3. Dust Age by Deposition Processes

[28] Not only does dust deposited have different ages from dust aloft, dust deposited by wet and dry deposition have different ages (Table 1). The age of dry-deposited dust reflects the dust age near the surface while the age of wet-deposited dust represents the mass-average dust age in higher layers where precipitation originates. Since the age of dust aloft increases with altitude, dust aloft and wet-deposited dust are much older than dry-deposited dust for all dust size ranges. Dust aloft is slightly older than wet-deposited dust for submicron dust and younger for larger dust. Since dust deposition is dominated by dry deposition for larger particles (size bin 3 and 4) and by wet deposition for smaller particles (size bin 1 and 2), the age of deposited

dust is determined by the age of dry-deposited dust for size bins 3 and 4 and by the age of wet-deposited dust for size bins 1 and 2. Thus deposited dust is usually younger than dust aloft except for size bin 2.

[29] The global mass of dust in each size class is binned in days according to age (Figure 5). Although dust ages range from hours to years, most dust (by mass) is younger than 2 weeks. 90% of wet-deposited dust is younger than twice the global average age of wet-deposited dust and 90% of dry-deposited dust is younger than three times the average dry-deposited dust age. Large dust particles are concentrated in younger ages while small dust size bins have a relatively flat distribution curve. Dry-deposited dust is more concentrated in short ages than is wet-deposited dust. The portion of dust aloft aged less than 20 days is between the two kinds of deposited dust but more dust aloft is older than 25 days due to the influence of (very old) stratospheric dust.

[30] The average age of wet-deposited dust is almost twice that of the dry-deposited dust, but their age distributions have very similar spatial patterns (Figures 2c–2f).

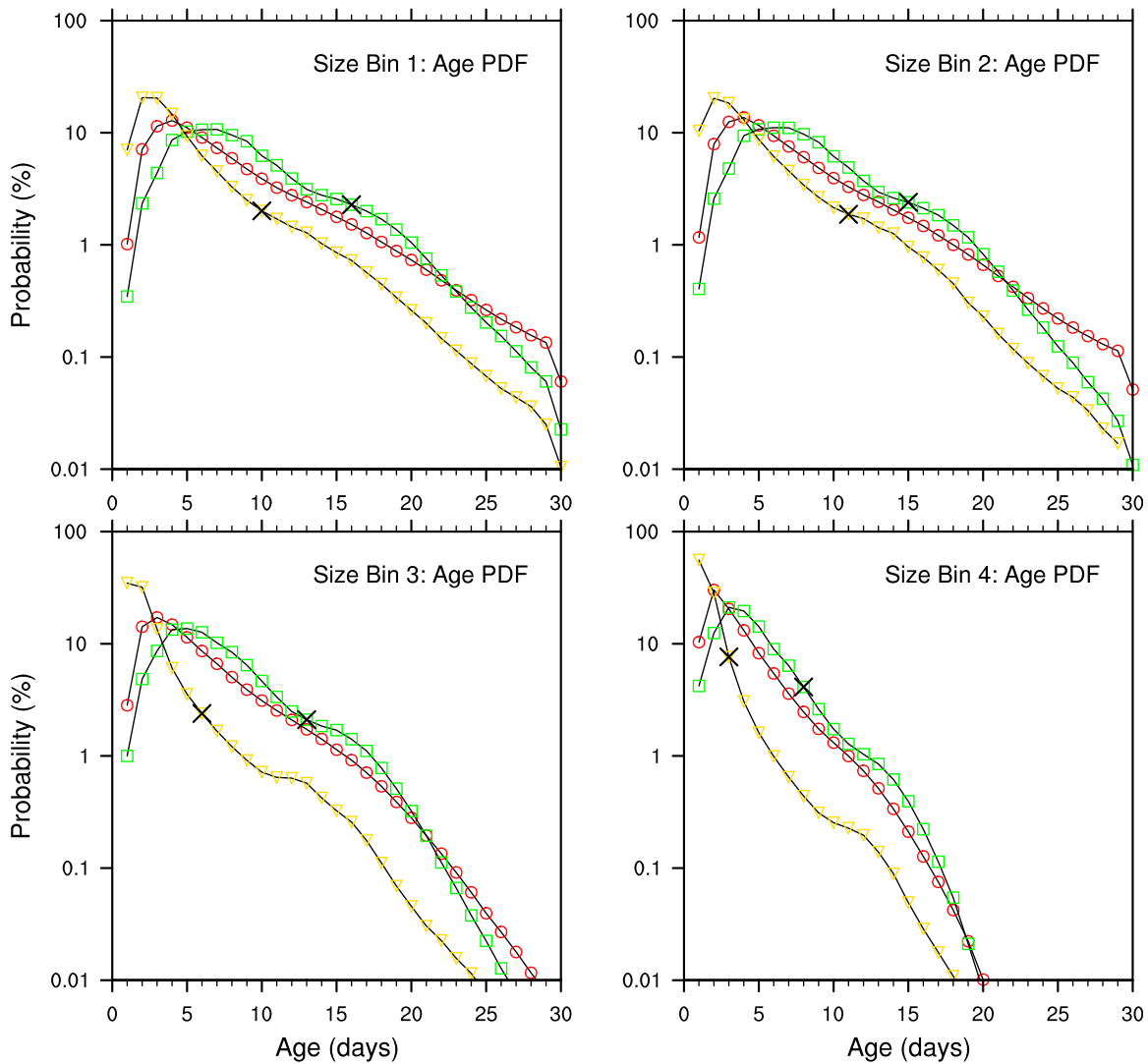


Figure 5. The age probability distributions of dust. Red circles for dust in the atmosphere, green squares for wet-deposited dust, and yellow triangles for dry-deposited dust. The crosses denote that 90% of wet or dry deposited dust in mass have ages younger than the ages at the crosses.

Most regions have deposited dust older than the global average dust age. For dry-deposited dust, only dust deposited in deserts has age near the global average dust age. Again, since we are calculating the mass-weighted age, the desert regions count for more than half of the global total dust deposition and thus dominate the global average age of deposited dust.

4. Discussion

[31] We developed the mass-age tracking (MAT) method as an efficient and accurate means of estimating the mass-weighted age of tracers. For this particular purpose, MAT has many advantages over other experimental and modeling tracer age estimation methods. MAT does not depend on age proxies and thus tracks mass-weighted tracer ages accurately at any location and any time. MAT can be applied to any mass-conserving tracer (e.g., aerosol, gas, isotope, chemical) in geophysical models. Unlike related

tracer age methods [e.g., *Thiele and Sarmiento, 1990; England, 1995; Neu and Plumb, 1999*], MAT does not require new prognostic equations and processes to track age; instead MAT slightly modifies the prognostic equation for mass (equation (1)) and solves it for mass-age (equation (2)). Thus, MAT embeds rather naturally in GCMs and CTMs, where it may be implemented as a second call to all the mass-transformative algorithms.

[32] Whereas the TTPDF method [*Holzer and Hall, 2000*] tracks a full spectrum of age PDFs and is appropriate for studies that need age distributions inside each grid cell, MAT tracks only one mass-weighted age at one grid cell for each tracer. For each tracer species, MAT consumes computer time equal to that required to simulate the lifecycle of the tracer. In our case of tracking four aerosols in a tropospheric GCM, MAT increased total simulation time by 25%. MAT can also be modified for other uses, e.g., examining the age influence of each aerosol lifecycle process, or estimating the fractions of tracers traversing particular regions.

[33] We applied the MAT method to four sizes of dust aerosols ranging from 0.1 to 10.0 μm in diameter. The results provide insights into the roles of transport, deposition processes and meteorology on dust age. Climate, mostly wind and precipitation, have a large impact on dust age, especially for smaller dust particles. The global average dust ages at deposition range between 1.4 and 7.8 days in the current climate. In the same climate, dust age varies with location, time and particle size. Dust that is further from its origin, higher, or smaller, is likely to be older than otherwise. Larger dust in summer is clearly older than in winter, but there is no obvious annual pattern for smaller dust. While fine dust lofted into the stratosphere may remain there for years, over 90% of dust deposits within 2 weeks.

[34] We presented the first global distribution maps of aerosol age. With the distribution of aerosol ages, aerosol properties and lifecycles can be further examined, understood and accounted for. For example, aerosols experience chemical processing during transport and comparisons between chemical models and observations show that older dust may be more soluble because it has experienced more or longer exposure to sunlight, clouds, and heterogeneous chemistry [Hand et al., 2004]. Thus ocean areas far from dust source regions could receive dust with a solubility that is larger than the global average and therefore more soluble iron could be delivered to these low dust deposition regions than estimated by globally uniform solubilities [Moore et al., 2004; Han et al., 2008]. Conversely, oceans immediately downwind of deserts may receive dust that is less soluble [Baker et al., 2006]. The MAT method may be a useful means of accounting such age-related consequences in large-scale models.

[35] **Acknowledgments.** This research was supported by NSF OCE-0452972, NSF ARC-0714088, and NASA NNX07AR23G. We thank F. Primeau and three anonymous reviewers for suggestions and helpful comments.

References

- Baker, A. R., T. D. Jickells, M. Witt, and K. L. Linge (2006), Trends in the solubility of iron, aluminium, manganese and phosphorus in aerosol collected over the Atlantic Ocean, *Mar. Chem.*, *98*, 43–58.
- Buck, C. S., W. M. Landing, J. A. Resing, and C. I. Measures (2008), The solubility and deposition of aerosol Fe and other trace elements in the North Atlantic Ocean: Observations from the A16N CLIVAR/CO₂ repeat hydrography section, *Mar. Chem.*, doi:10.1016/j.marchem.2008.08.003.
- Collins, W. D., P. J. Rasch, B. A. Boville, J. J. Hack, J. R. McCaa, D. L. Williamson, J. T. Kiehl, and B. Briegleb (2004), Description of the NCAR community atmosphere model (CAM 3.0), *Tech. Rep. NCAR TN-464+STR*, Natl. Cent. for Atmos. Res., Boulder, Colo.
- England, M. H. (1995), The age of water and ventilation time scales in a global ocean model, *J. Phys. Oceanogr.*, *25*, 2756–2777.
- Flanner, M. G., C. S. Zender, J. T. Randerson, and P. J. Rasch (2007), Present-day climate forcing and response from black carbon in snow, *J. Geophys. Res.*, *112*, D11202, doi:10.1029/2006JD008003.
- Hall, T. M., and R. A. Plumb (1994), Age as a diagnostic of stratospheric transport, *J. Geophys. Res.*, *99*(D1), 1059–1070, doi:10.1029/93JD03192.
- Han, Q., J. K. Moore, C. Zender, C. Measures, and D. Hydes (2008), Constraining oceanic dust deposition using surface ocean dissolved Al, *Global Biogeochem. Cycles*, *22*, GB2003, doi:10.1029/2007GB002975.
- Hand, J. L., N. M. Mahowald, Y. Chen, R. L. Siefert, C. Luo, A. Subramaniam, and I. Fung (2004), Estimates of atmospheric-processed soluble iron from observations and a global mineral aerosol model: Biogeochemical implications, *J. Geophys. Res.*, *109*, D17205, doi:10.1029/2004JD004574.
- Holzer, M., and T. M. Hall (2000), Transit-time and tracer-age distributions in geophysical flows, *J. Atmos. Sci.*, *57*, 3539–3558.
- Holzer, M., I. G. McKendry, and D. A. Jaffe (2003), Springtime trans-Pacific atmospheric transport from east Asia: A transit-time probability density function approach, *J. Geophys. Res.*, *108*(D22), 4708, doi:10.1029/2003JD003558.
- Kleinman, L. I., et al. (2003), Photochemical age determinations in the Phoenix metropolitan area, *J. Geophys. Res.*, *108*(D3), 4096, doi:10.1029/2002JD002621.
- Krinner, G., and C. Genthon (2003), Tropospheric transport of continental tracers towards Antarctica under varying climatic conditions, *Tellus, Ser. B*, *55*, 54–70.
- Krishnamurthy, A., J. K. Moore, N. Mahowald, C. Luo, S. C. Doney, K. Lindsay, and C. S. Zender (2009), Impacts of increasing anthropogenic soluble iron and nitrogen deposition on ocean biogeochemistry, *Global Biogeochem. Cycles*, *23*, GB3016, doi:10.1029/2008GB003440.
- Kuroda, P. K., H. L. Hodges, L. M. Fry, and H. E. Moore (1962), Stratospheric residence time of Strontium-90, *Science*, *137*(3523), 15–17.
- Luo, C., N. M. Mahowald, N. Meskhidze, Y. Chen, R. L. Siefert, A. R. Baker, and A. M. Johansen (2005), Estimation of iron solubility from observations and a global aerosol model, *J. Geophys. Res.*, *110*, D23307, doi:10.1029/2005JD006059.
- Luo, C., N. Mahowald, T. Bond, P. Y. Chuang, P. Artaxo, R. Siefert, Y. Chen, and J. Schauer (2008), Combustion iron distribution and deposition, *Global Biogeochem. Cycles*, *22*, GB1012, doi:10.1029/2007GB002964.
- Mahowald, N. M., D. R. Muhs, S. Levis, P. J. Rasch, M. Yoshioka, C. S. Zender, and C. Luo (2006), Change in atmospheric mineral aerosols in response to climate: Last glacial period, preindustrial, modern, and doubled carbon dioxide climates, *J. Geophys. Res.*, *111*, D10202, doi:10.1029/2005JD006653.
- McKeen, S. A., and S. C. Liu (1993), Hydrocarbon rotios and photochemical history of air masses, *Geophys. Res. Lett.*, *20*(21), 2363–2366, doi:10.1029/93GL02527.
- Moore, J. K., S. C. Doney, and K. Lindsay (2004), Upper ocean ecosystem dynamics and iron cycling in a global three-dimensional model, *Global Biogeochem. Cycles*, *18*, GB4028, doi:10.1029/2004GB002220.
- Neu, J. L., and R. A. Plumb (1999), Age of air in a “leaky pipe” model of stratospheric transport, *J. Geophys. Res.*, *104*(D16), 19,243–19,255, doi:10.1029/1999JD900251.
- Parrish, D. D., C. J. Hahn, E. J. Williams, R. B. Norton, F. C. Fehsenfeld, H. B. Singh, J. D. Shetter, B. W. Gandrud, and B. A. Ridley (1993), Reply, *J. Geophys. Res.*, *98*(D8), 14,995–14,997, doi:10.1029/93JD01416.
- Poet, S. E., H. E. Moore, and E. A. Martell (1972), Lead 210, Bismuth 210, and Polonium 210 in the atmosphere: accurate ration measurement and application to aerosol residence time determination, *J. Geophys. Res.*, *77*(33), 6515–6527, doi:10.1029/JC077i033p06515.
- Prather, M. J. (2007), Lifetimes and time scales in atmospheric chemistry, *Philos. Trans. R. Soc.*, *365*, 1705–1726.
- Primeau, F. W., and M. Holzer (2006), The ocean’s memory of the atmosphere: Residence-time and ventilation-rate distributions of water masses, *J. Phys. Oceanogr.*, *36*, 1439–1456.
- Rasch, P. J., D. B. Coleman, N. Mahowald, and D. L. Williamson (2006), Characteristics of atmospheric transport using three numerical formulations for atmospheric dynamics in a single GCM framework, *J. Clim.*, *19*(11), 2243–2266.
- Roberts, J., F. Fehsenfeld, and S. Liu (1984), Measurements of aromatic hydrocarbon ratios and NO_x concentrations in the rural troposphere - observation of air mass photochemical aging and NO_x removal, *Atmos. Environ.*, *18*(11), 2421–2432.
- Rudolph, J., and E. Czuba (2000), On the use of isotopic composition measurements of volatile organic compounds to determine the “photochemical age” of an air mass, *Geophys. Res. Lett.*, *27*(23), 3865–3868, doi:10.1029/2000GL011385.
- Seinfeld, J. H., and S. N. Pandis (2006), *Atmospheric Chemistry and Physics*, 2nd ed., John Wiley, Hoboken, N. J.
- Spokes, L. J., and T. D. Jickells (1996), Factors controlling the solubility of aerosol trace metals in the atmosphere and on mixing into seawater, *Aquat. Geochem.*, *1*, 355–374.
- Stohl, A., et al. (2003), A backward modeling study of intercontinental pollution transport using aircraft measurements, *J. Geophys. Res.*, *108*(D12), 4370, doi:10.1029/2002JD002862.
- Thiele, G., and J. L. Sarmiento (1990), Tracer dating and ocean ventilation, *J. Geophys. Res.*, *95*(C6), 9377–9391, doi:10.1029/JC095iC06p09377.
- Wagstrom, K. M., and S. N. Pandis (2009), Determination of the age distribution of primary and secondary aerosol species using a chemical transport model, *J. Geophys. Res.*, *114*, D14303, doi:10.1029/2009JD011784.
- Waugh, D. W., T. M. Hall, and T. W. N. Haine (2003), Relationship among tracer ages, *J. Geophys. Res.*, *108*(C5), 3138, doi:10.1029/2002JC001325.

Williamson, D. L., and P. J. Rasch (1994), Water-vapor transport in the NCAR-CCM2, *Tellus, Ser. A*, 46(1), 34–51.

Zender, C. S., H. Bian, and D. Newman (2003), Mineral Dust Entrainment and Deposition (DEAD) model: Description and 1990s dust climatology, *J. Geophys. Res.*, 108(D14), 4416, doi:10.1029/2002JD002775.

Zender, C. S., R. L. Miller, and I. Tegen (2004), Quantifying mineral dust mass budgets: Terminology, constraints, and current estimates, *Eos Trans. AGU*, 85(48), 509–512.

Q. Han and C. S. Zender, Department of Earth System Science, University of California, Irvine, CA 92697-3100, USA. (zender@uci.edu)